

Supplement of Geosci. Model Dev. Discuss., 8, 5671–5739, 2015  
<http://www.geosci-model-dev-discuss.net/8/5671/2015/>  
doi:10.5194/gmdd-8-5671-2015-supplement  
© Author(s) 2015. CC Attribution 3.0 License.



*Supplement of*

## **Development and evaluation of CNRM Earth-System model – CNRM-ESM1**

**R. Sférian et al.**

*Correspondence to:* R. Sférian (roland.seferian@meteo.fr)

The copyright of individual parts of the supplement might differ from the CC-BY 3.0 licence.

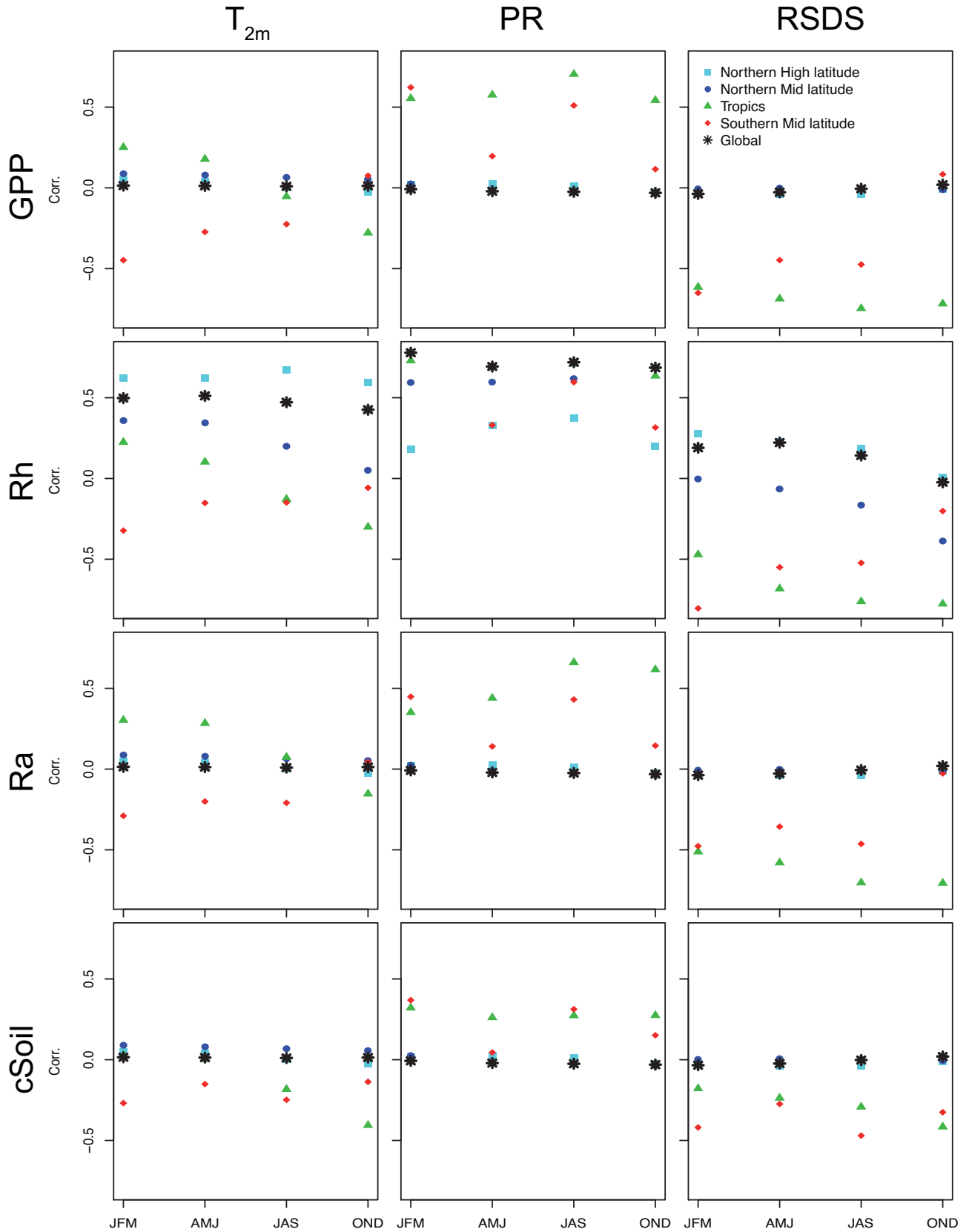


Figure 1: Spatial correlation between land carbon cycle parameters and physical drivers. Land carbon cycle parameters are the growth primary productivity (GPP), autotrophic and heterotrophic respiration (Ra and Rh, respectively) and the stock of soil carbon (cSoil). The physical drivers are the near-surface air temperature ( $T_{2m}$ ), precipitation (PR) and incoming shortwave radiation (RSDS). Correlation is computed at global scale (star symbol) and over Northern High latitude (square), Northern Mid latitude (circle), tropics (triangle) and Southern Mid latitude (diamond) between fields averaged over the four seasons (JFM, AMJ, JAS, OND) from 1986 to 2005.

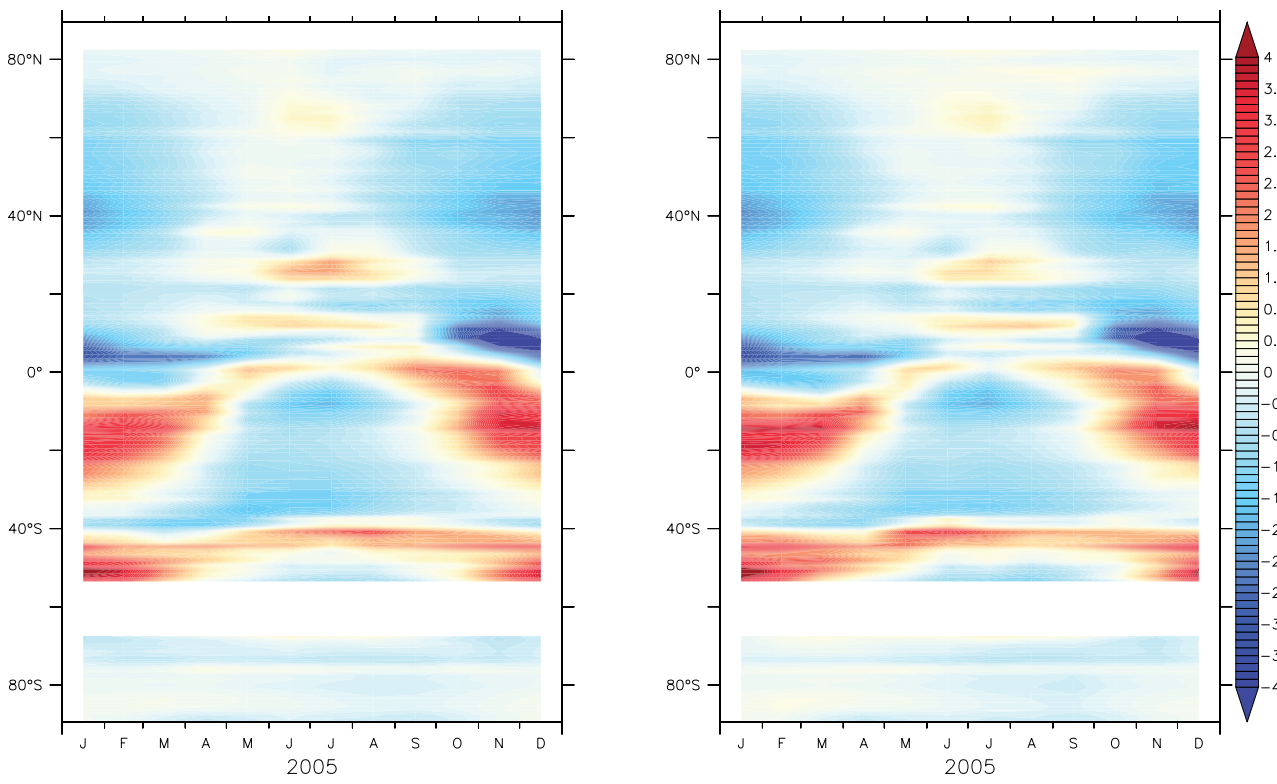


Figure 2: Seasonal variation of continental precipitation anomaly as simulated by CNRM-CM5.2 (left panel) and CNRM-ESM1 (right panel).

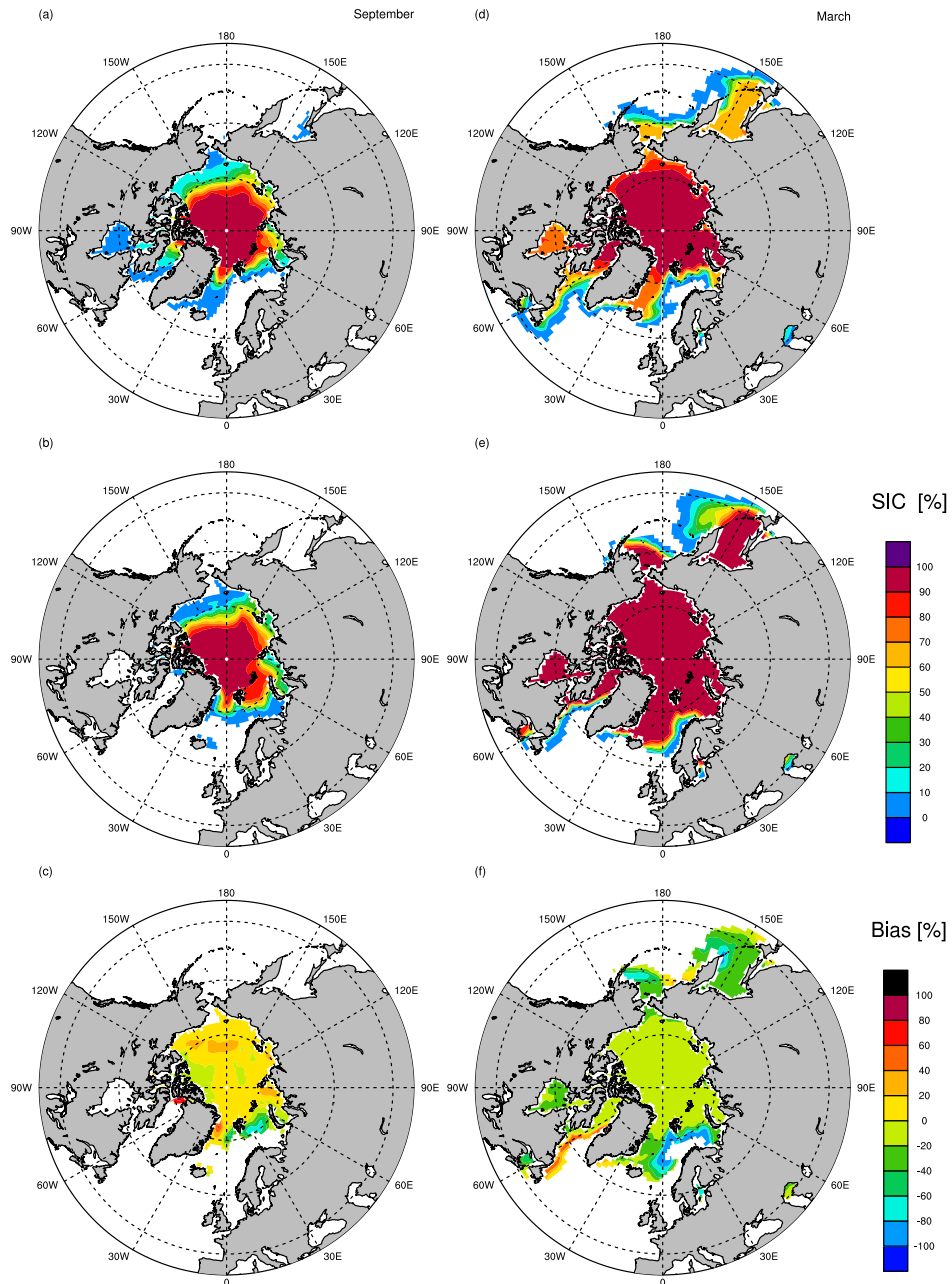


Figure 3: Impact of coupling frequency on the Arctic sea-ice cover (SIC) over the last 50 years of the preindustrial control simulation. Arctic SIC is represented at 24-hour coupling frequency for September (a) and March (d), and at 6-hour coupling frequency for September (b) and March (e). Differences in Arctic SIC attributed to change in coupling frequency are represented for September (c) and March (f).

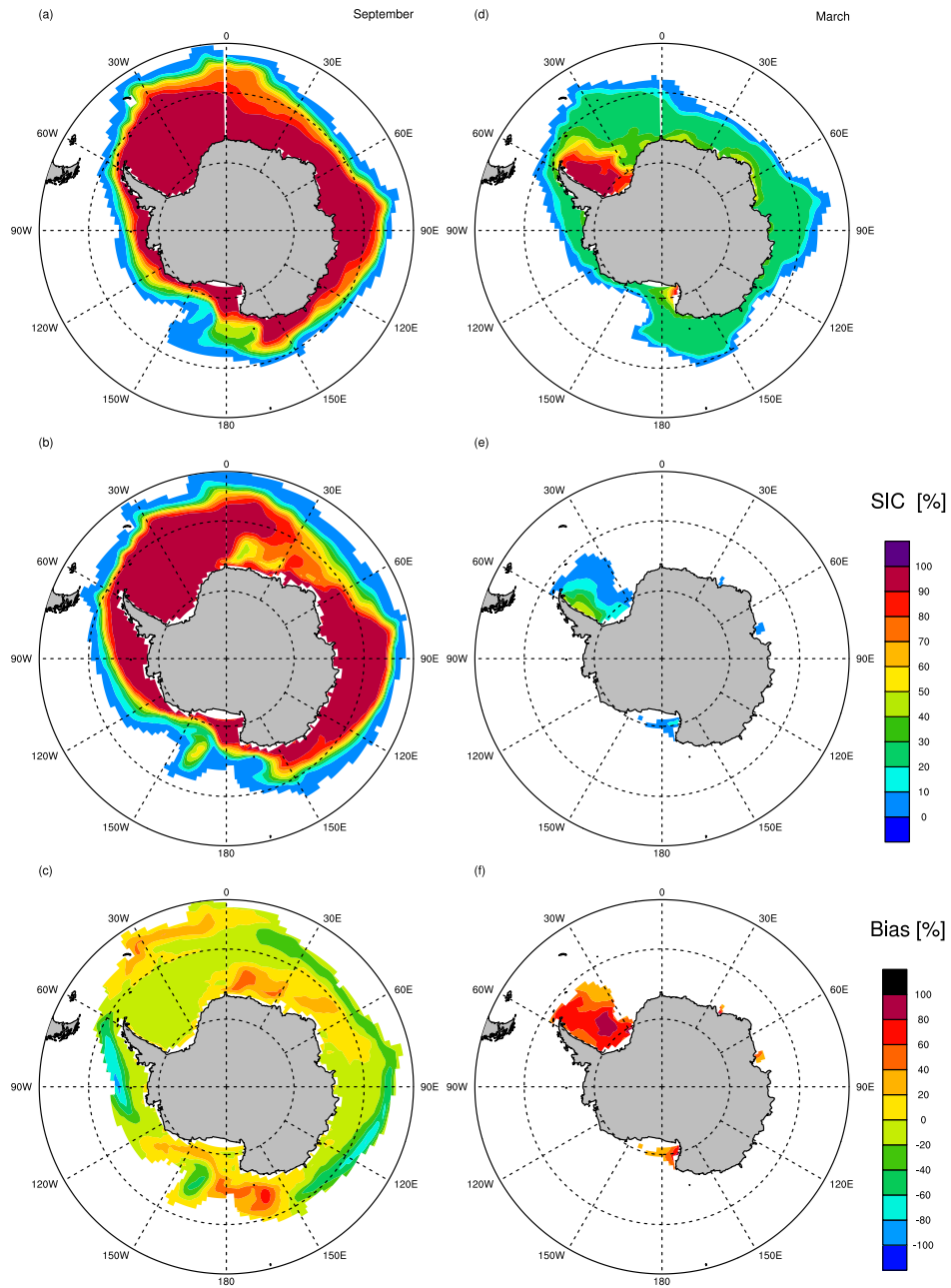


Figure 4: Impact of coupling frequency on the Antarctic sea-ice cover (SIC) over the last 50 years of the preindustrial control simulation. Antarctic SIC is represented at 24-hour coupling frequency for September (a) and March (d), and at 6-hour coupling frequency for September (b) and March (e). Differences in Antarctic SIC attributed to change in coupling frequency are represented for September (c) and March (f).

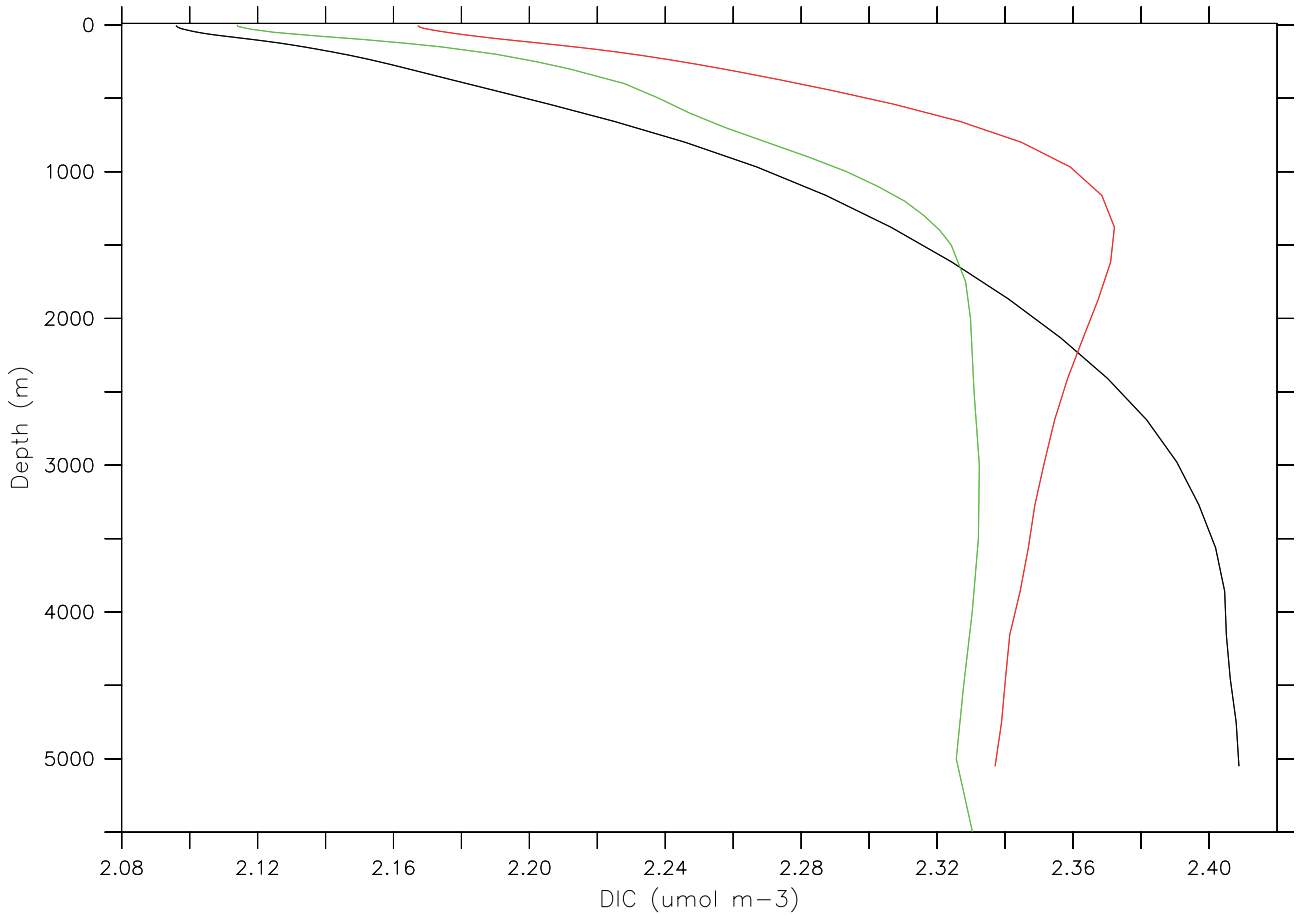


Figure 5: Vertical profiles of dissolved inorganic carbon concentration averaged over the Southern Ocean (South of  $30^\circ$ ) as simulated by CNRM models and provided by GLODAP observation (Key et al., 2004). Observations, CNRM-CM5.2 (Séférian et al., 2013) and CNRM-ESM1 profiles are represented by green, black and red solid lines. Observations use 1994 as single reference year, whilst model results have been averaged over 1986-2005.

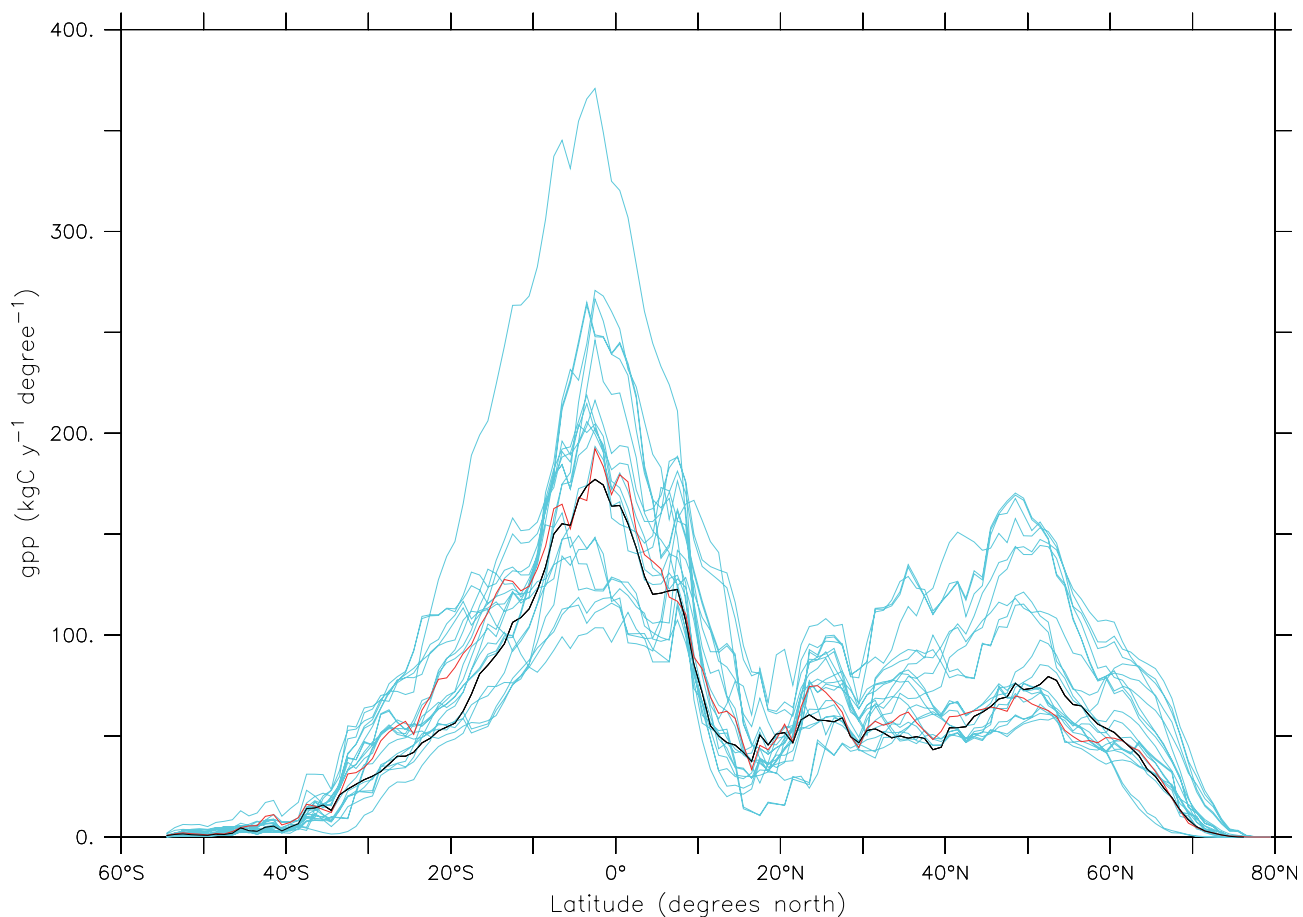


Figure 6: Zonally-cumulated gross primary productivity (gpp) averaged over 1986-2005 from observation-derived estimates and as estimated by CMIP5 Earth system models (ESMs) plus CNRM-ESM1. Observation-derived estimates from FluxNet-MTE (Jung et al., 2011) are represented with a solid black line. Result from CNRM-ESM1 is given with a solid red line, while those of the various CMIP5 ESMs are indicated with solid blue lines. This ensemble of CMIP5 ESMs accounts for results from bcc-csm1-1, BNU-ESM, CanESM2, inmcm4, IPSL-CM5A-LR, IPSL-CM5A-MR, IPSL-CM5B-LR, MIROC-ESM-CHEM, MIROC-ESM, HadGEM2-CC, HadGEM2-ES, MPI-ESM-LR, MPI-ESM-MR, MRI-ESM1, GISS-E2-H-CC, GISS-E2-R-CC, GISS-E2-R, NorESM1-ME, GFDL-ESM2G, GFDL-ESM2M and CESM1-BGC.

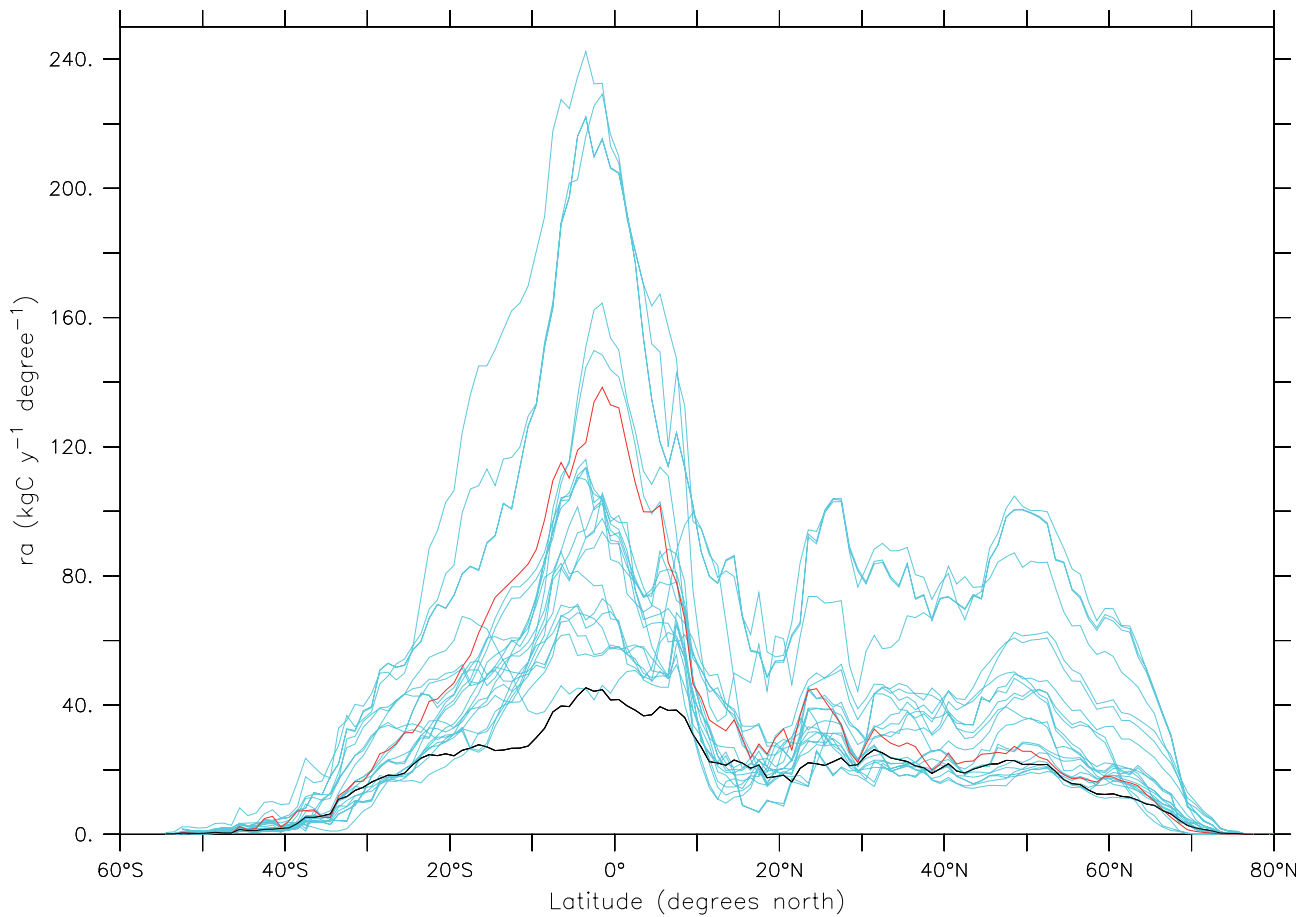


Figure 7: Zonally-cumulated autotrophic respiration ( $ra$ ) averaged over 1986-2005 from observation-derived estimates and as estimated by CMIP5 Earth system models (ESMs) plus CNRM-ESM1. Observation-derived estimates from Hashimoto et al. (2015) are represented with a solid black line. Result from CNRM-ESM1 is given with a solid red line, while those of the various CMIP5 ESMs are indicated with solid blue lines. This ensemble of CMIP5 ESMs accounts for results from bcc-csm1-1, BNU-ESM, CanESM2, inmcm4, IPSL-CM5A-LR, IPSL-CM5A-MR, IPSL-CM5B-LR, MIROC-ESM-CHEM, MIROC-ESM, HadGEM2-CC, HadGEM2-ES, MPI-ESM-LR, MPI-ESM-MR, MRI-ESM1, GISS-E2-H-CC, GISS-E2-R-CC, GISS-E2-R, NorESM1-ME, GFDL-ESM2G, GFDL-ESM2M and CESM1-BGC.



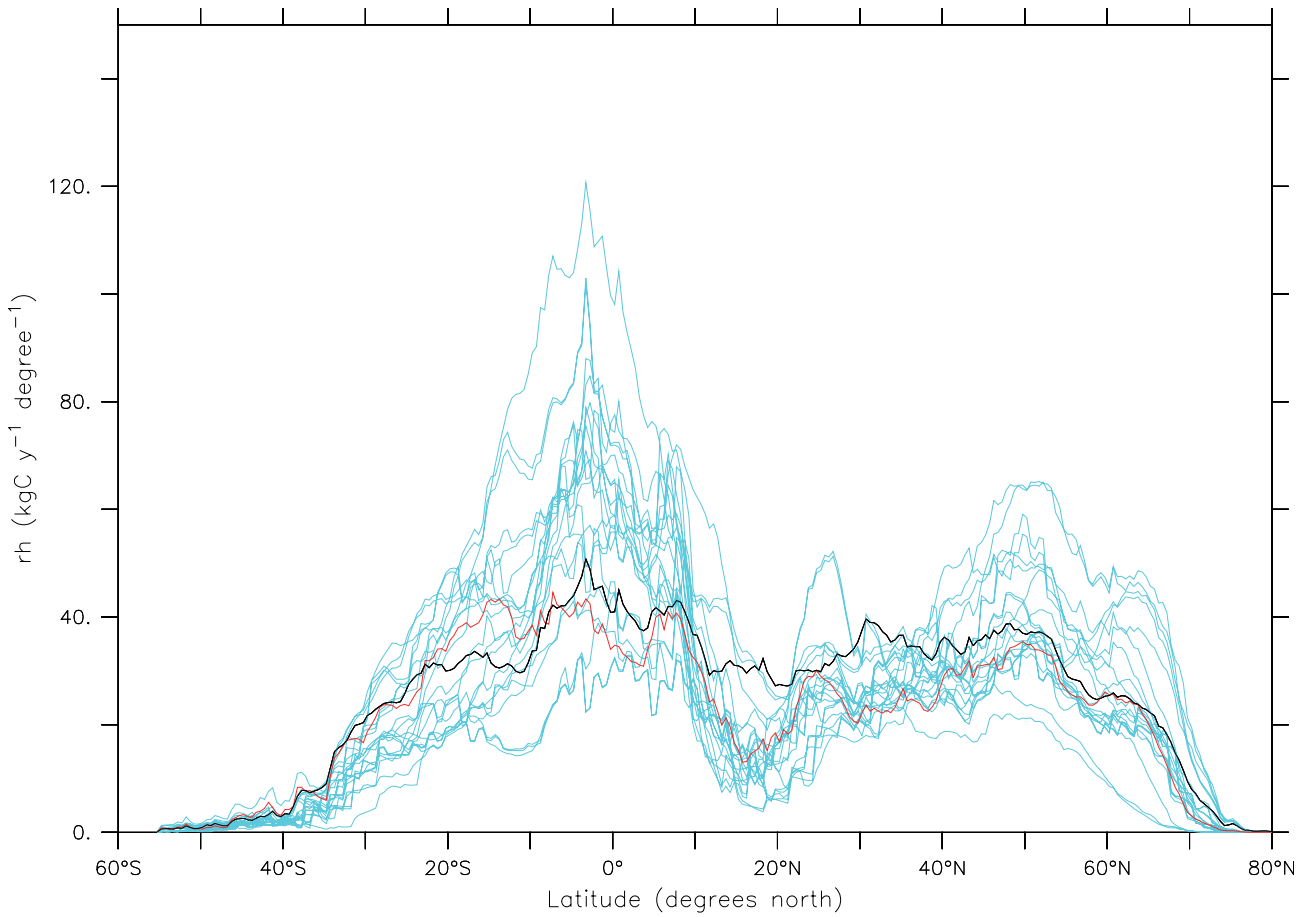


Figure 8: Zonally-cumulated heterotrophic respiration (rh) averaged over 1986-2005 from observation-derived estimates and as estimated by CMIP5 Earth system models (ESMs) plus CNRM-ESM1. Observation-derived estimates from Hashimoto et al. (2015) are represented with a solid black line. Result from CNRM-ESM1 is given with a solid red line, while those of the various CMIP5 ESMs are indicated with solid blue lines. This ensemble of CMIP5 ESMs accounts for results from bcc-csm1-1, BNU-ESM, CanESM2, inmcm4, IPSL-CM5A-LR, IPSL-CM5A-MR, IPSL-CM5B-LR, MIROC-ESM-CHEM, MIROC-ESM, HadGEM2-CC, HadGEM2-ES, MPI-ESM-LR, MPI-ESM-MR, MRI-ESM1, GISS-E2-H-CC, GISS-E2-R-CC, GISS-E2-R, NorESM1-ME, GFDL-ESM2G, GFDL-ESM2M and CESM1-BGC.